(4) Hashimoto, T.; Toda, A.; Itoi, H.; Kawai, H. *Macromolecules* **1977**, *10*, 377.
(5) Hashimito, T.; Shibayama, M.; Kawai, H. *Macromolecules* **1980**, *13*, 1237.
(6) Vanzo, E. J. *J. Polym. Sci.* **1966**, *A4*, 1727.
(7) Bradford, E. B.; Vanzo, E. *J. Polym. Sci.* **1986**, *A1*, 1661.
(8) Whitmann, J. C.; Lotz, B.; Candau, F.; Kovacs, A. J. *J. Polym. Sci. Polym. Phys. Ed.* **1982**, *20*, 1341.
(9) Schmitt, R. L.; Gardella, J. A.; Magill, J. H.; Salvati, L.; Chin, R. L. *Macromolecules* **1985**, *18*, 2675.
(10) Thomas, H. R.; O'Malley, J. J. *Macromolecules* **1979**, *12*, 323.
(11) Green, P. F.; Christensen, T. M.; Russell, T. P.; Jérôme, R. *Macromolecules*, **1989**, *22*, 2189.
(12) Coulon, G.; Russell, T. P.; Deline, V.; Green, P. F. *Macromolecules* **1989**, *22*, 2581.
(13) Green, P. F.; Russell, T. P.; Jérôme, R., Granville, M. *Macromolecules* **1988**, *21*, 3266.
(14) Russell, T. P.; Jérôme, R, unpublished results.
(15) Coulon, G.; Aussêré, D.; Russell, T. P., submitted for publication in *Macromolecules*.
(16) Green, P. F.; Christensen, T.; Russell, T. P.; Jérôme, R. *J. Chem. Phys.*, in press.
(17) Russell, T. P.; Hjelm, R.; Seeger, P. *Macromolecules*, in press.
(18) Anastasiadis, S. H.; Russell, T. P.; Satija, S. K.; Majkrazak, C. F. *Phys. Rev. Lett.* **1989**, *62*, 1852.
(19) Shibayama, M.; Hashimoto, T.; Hasegawa, H.; Kawai, H. *Macromolecules* **1983**, *16*, 1427.
(20) Meier, D. J. In *Thermoplastic Elastomers—Research and Development*; Legge, N. R., Holden, G., Schroeder, H., Eds.; Hansen Publishing: Munich, 1988.

Neutron Scattering Studies of Blends of Poly(2,6-dimethyl-1,4-phenylene oxide) with Poly(4-methylstyrene) and with Polystyrene: Concentration and Temperature Dependence

Ann Maconnachie,*,† J. R. Fried,‡ and Paul E. Tomlins§

Department of Chemical Engineering and Chemical Technology, Imperial College of Science, Technology, and Medicine, Prince Consort Road, London SW7 2BY, U.K., Department of Chemical Engineering, University of Cincinnati, Cincinnati, Ohio 45221-0171, and DMA Building 95, National Physical Laboratory, Teddington, Middlesex TW11 0LW, U.K. *Received October 25, 1988; Revised Manuscript Received April 27, 1989*

ABSTRACT: Quenched samples of binary blends of polystyrene, PS, and of poly(4-methylstyrene), P4MS, with poly(2,6-dimethyl-1,4-phenylene oxide), PM2PO, have been studied using small-angle neutron scattering, SANS. The composition and temperature dependences of the interaction parameter, χ, and the radius of gyration, R, of PS and P4MS in PM2PO have been measured. No evidence of chain expansion of either PS or P4MS in PM2PO was observed. The interaction parameters, measured in the q range 2×10^{-2}–4×10^{-2} Å^{-1} (where q is the scattering vector), appear to be independent of annealing temperature. This has been interpreted as indicating that over short distance scales the blends equilibrate at temperatures close to their glass transition temperature. For PS/PM2PO blends, χ follows the temperature dependence suggested by mutual diffusion measurements, which assume that it is independent of composition. The values of χ for the P4MS/PM2PO blends are thermodynamically poorer than those of the PS/PM2PO blends.

The range of known miscible polymer pairs grows daily even though until quite recently it was considered highly unusual for high polymers to mix. Why two polymers might or might not mix can be explained by recourse to the thermodynamics of polymer mixtures. In order to achieve a favorable free energy of mixing, it is usually necessary to also have a favorable heat of mixing since the entropy of mixing is essentially zero for high polymers. Unless there is a specific interaction or favorable volume change, the polymers are unlikely to mix. Mixtures of polystyrene (PS) and poly(2,6-dimethyl-1,4-phenylene oxide) (PM2PO) form miscible single-phase materials in all proportions, and although lower critical solution temperature (LCST) behavior has been indicated,[1-3] phase separation has not been achieved at reasonable temperatures. The PS/PM2PO system has been closely studied, particularly the effect of changing the thermodynamic interactions in the system by substituting halogen atoms into the phenyl or phenylene ring of the polymers.[4-7] The position, number, and size of the halogens have been varied, and the effect on the miscibility of the polymer pairs was reported. Monosubstituted PS, either ortho- or para-substituted with chlorine or fluorine, is immiscible with PM2PO.[4-6] Monosubstituted PM2PO, with bromine in the 3-position, is also immiscible with PS.[7] However, if the substituent in the PS phenyl ring is changed to a methyl group, the effect is much less dramatic, and now the system becomes partially miscible.[8,9] The aim of this work is to compare the thermodynamics of the two blends PS/PM2PO and poly(4-methylstyrene) (P4MS)/PM2PO by measuring the interaction parameter, χ, as a function of composition and temperature. The technique that has been used is small-angle neutron scattering (SANS).

Table I
Characterization Data

	M_w[a]	M_w/M_n[a]	N_w[b]
PS	300 000	2.52	2884
PS-*d*	379 000	2.94	3486
P4MS	80 900	1.09	686
P4MS-*d*	88 500	1.73	708
PM2PO	35 400	1.62	295

[a] Measured by GPC from universal calibration of 10 PS standards in toluene. [b] Degree of polymerization.

Experimental Section

1. **Materials and Sample Preparation.** Poly(4-methylstyrene) and ring-deuterated poly(4-methylstyrene-d_7) (P4MS-*d*) were supplied through the courtesy of Dr. B. Z. Gunesin of the Mobil Chemical Co. Polystyrene was obtained from BASF and ring-deuterated polystyrene-d_5 (PS-*d*) from Cambridge Isotope

† Imperial College of Science, Technology, and Medicine.
‡ University of Cincinnati.
§ National Physical Laboratory.

0024-9297/89/2222-4606$01.50/0

Table II
Sample Compositions with Details of ϕ (Volume Fractions) and c (Proportion of Deuterated Chains)

sample no.	ϕ_{PM2PO}	ϕ_{PS-d}	ϕ_{P4MS-d}	ϕ_{PS}	ϕ_{P4MS}	c
		Series 1. χ Parameter				
31	0.906	0.094				1
19	0.811	0.189				1
32	0.712	0.288				1
17	0.619	0.381				1
15	0.416	0.584				1
33	0.899		0.101			1
8	0.802		0.198			1
34	0.699		0.301			1
6	0.601		0.399			1
4	0.400		0.600			1
		Series 2. Single Chain				
21		0.092		0.908		0.096
14	0.198	0.068		0.733		0.088
16	0.398	0.051		0.551		0.088
18	0.598	0.033		0.369		0.086
20	0.798	0.018		0.184		0.090
11			0.100		0.900	0.100
5	0.389		0.126		0.485	0.205
7	0.590		0.083		0.326	0.203
9	0.791		0.043		0.166	0.204

Laboratories. Poly(2,6-dimethyl-1,4-phenylene oxide) was supplied by the General Electric Co. The PM2PO was subsequently fractionated from toluene solution using methanol. Details of molecular weights and polydispersities are given in Table I.

The polymer mixtures were prepared by codissolution in benzene followed by freeze-drying. The resulting powders were dried further under vacuum at approximately 70 °C overnight. Disks of the blends approximately 16 mm in diameter and 0.5–1 mm thick were produced by compression moulding each powder above its glass transition temperature. Two series of mixtures were made for each blend system: (1) mixtures of PS-*d* and PM2PO or P4MS-*d* and PM2PO in which the concentration of deuterated polymer was varied, and (2) three-component mixtures of PS-*d*/PS/PM2PO or P4MS-*d*/P4MS/PM2PO where the proportion of PS-*d* (or P4MS-*d*) to PS (or P4MS) was kept constant (see Theory). Table II gives details of the compositions of the samples. The moulded disks were then put into an aluminium holder, which was sandwiched between 1-mm-thick stainless steel plates using a G-clamp. This whole assembly was then heated in an oven under nitrogen to anneal the samples. Annealing times varied depending upon the relative values of the annealing temperature and the glass transition temperature (T_g) of the blend. The assembly containing the sample was then dropped into cold water to quench the samples as rapidly as possible. The annealing temperatures varied from 220 to 280 °C. Samples of each disk were subjected to differential scanning calorimetry using a Perkin Elmer DSC-7. All samples exhibited one glass transition temperature indicative of a one-phase homogeneous mixture.

2. Small-Angle Neutron Scattering. (a) Experimental Details and Data Reduction. The SANS measurements were carried out at the Institut Laue-Langevin using the small-angle scattering diffractometers D11 and D17 (details of these instruments can be found in ref 10). All measurements were carried out at room temperature. Sample-to-detector distances and wavelengths used were 12 m and 8 Å and 3.5 m and 15 Å for D11 and D17, respectively. The q ranges covered were 3.3×10^{-3} Å^{-1} $< q < 2.3 \times 10^{-2}$ Å^{-1} and $6.0 \times 10^{-3} < q < 4.2 \times 10^{-2}$ Å^{-1}, respectively. ($q = 4\pi \sin(\theta/2)/\lambda$, where θ is the scattering angle and λ is the neutron wavelength.)

The scattering was measured from the following series of samples: (1) each blend or mixture; (2) the pure hydrogenous polymers; (3) the sample holder; (4) a 1-mm-thick water sample; (5) the water cell. The scattered intensity from items (1) and (2) was corrected for background scattering using (3) and for detector efficiency using (4) and (5) to give the corrected intensity, $I_c(q)$.

The incoherent scattering I_i was then subtracted from $I_c(q)$, as described below, and the data were normalized using the measured cross section of water,[11] $(d\sigma/d\Omega)_w^{1mm}$, to give the coherent scattering cross section of the blend, $(d\sigma/d\Omega)_{coh}$

$$(d\sigma/d\Omega)_{coh} = S(q) = [I_{c,s}(q) - I_{i,s}]\frac{d_w T_w}{d_s T_s}\left[\frac{d\sigma}{d\Omega}\right]_w^{1mm} \text{ (cm}^{-1}\text{)} \quad (1)$$

where d_w and T_w and d_s and T_s are the thickness and transmission of the water and sample, respectively. $I_{c,s}(q)$ and $I_{i,s}$ are the corrected intensity and the incoherent scattering from the sample (blend), respectively.

A number of methods have been used in the literature to estimate the level of incoherent scattering from a polymer sample.[12-14] The method advocated by Hayashi et al.[12] uses the calculated incoherent transmission of the sample, T_i^{calc}, and assumes that the incoherent scattering is proportional to $1 - T_i^{calc}$

$$T_i^{calc} = \exp(-\sigma_i^B n d) \quad (2)$$

where σ_i^B is the bound atom incoherent cross section, n is the number of scatterers per cubic centimeter, and d is the thickness of the sample. The drawback of this method is that σ_i^B as tabulated does not vary with wavelength, whereas measurements of σ_i for polymers have shown that there is a strong dependence on wavelength and temperature.[13,15] A simpler method of estimating the incoherent scattering is to use the measured transmission itself. This also leads to some errors in the estimation of the incoherent scattering; however, the errors are significantly less than those involved in using the method of Hayashi et al. Use of the measured transmission has the added advantage of being simple and easy to carry out. A similar method of estimating the incoherent scattering has been used by O'Reilly et al.[16]

The incoherent scattering has been calculated as a proportion of the scattering from a pure hydrogenous polymer, $I_{c,H}$, so that

$$I_{i,s} = BI_{c,H} \quad (3a)$$

where

$$B = (1 - T_s)/(1 - T_H) \quad (3b)$$

and T_H is the transmission of a pure hydrogenous polymer. $I_{i,s}$ is q-independent, $I_{c,H}$ having been taken as the average value of the scattering from a hydrogenous polymer over a number of values of q where the scattering was q-independent. The coherent scattering from the hydrogenous polymers has been assumed to be negligible compared to the large incoherent cross section. In this work, $I_{i,s}$ has been estimated by scaling the scattering from pure PM2PO. Similar results were obtained if the scattering from PS was used.

With use of eq 3, the two methods mentioned above of estimating the incoherent scattering have been compared to the measured incoherent cross section. Three sets of values of the transmissions in eq 3b have been used in the calculation of $I_{i,s}$: (1) the measured transmissions, T_s and T_H; (2) the incoherent transmissions $T_{i,s}^{meas}$ and $T_{i,H}^{meas}$ calculated from the measured transmissions; and (3) the incoherent transmissions $T_{i,s}^{calc}$ and $T_{i,H}^{calc}$, calculated using tabulated values of σ_i^B. The following method has been used to calculate the incoherent cross section, σ_i^{meas}, from the measured transmission, T

$$\sigma_T^{meas} = \frac{-\ln T}{nd} \quad (4)$$

where σ_T^{meas} is the measured total cross section, $n = \rho N_A/m$, ρ is the density, m is the molecular weight, and N_A is Avogadro's number. Hence

$$\sigma_i^{meas} = \sigma_T^{meas} - \sigma_c \quad (5)$$

where σ_c is the coherent cross section. The absorption cross section for all the polymers used in this work is negligible. Thus

$$T_i^{meas} = \exp\left[-\sigma_i^{meas}\frac{\rho d N_A}{m}\right] \quad (6)$$

The values of the measured and calculated transmissions and cross sections for PM2PO and two PS/PM2PO samples are listed in Table III. The values of the total cross sections calculated from the measured transmissions are considerably larger than the bound atom values and increase with increasing wavelength. T, the measured transmission, is approximately 2% smaller than T_i^{meas} for all the samples whereas T_i^{calc} is larger than T_i^{meas} and the difference varies from 7 to 26%. These differences are reflected

Table III
Comparison of the Methods of Calculating the Level of Incoherent Scattering from Transmission Measurements

sample	ϕ_D	λ, Å	meas transmssn T	meas total cross section $\sigma_T \times 10^{24}$, cm^2	coherent cross section $(4\pi b^2)$ $\sigma_c \times 10^{24}$, cm^2	meas[a] incoherent cross section $\sigma_i \times 10^{24}$, cm^2	bound atom incoherent cross section $\sigma_i^B \times 10^{24}$, cm^2	$T_i^{calc\,b}$	$T_i^{meas\,c}$	$\frac{1-T_s}{1-T_H}$	$\frac{1-T_{i,s}^{meas}}{1-T_{i,H}^{meas}}$	$\frac{1-T_{i,s}^{calc}}{1-T_{i,H}^{calc}}$
PM2PO	0	8	0.686	992.1	62.40	929.7	637.92	0.785	0.702			
PM2PO	0	15	0.608	1309.8	62.40	1247.4	637.92	0.785	0.623			
20	0.018	8	0.716	1209.7	61.89	1147.8	630.92	0.840	0.728	0.904	0.913	0.744
20	0.018	15	0.680	1491.2	61.89	1429.3	630.92	0.849	0.691	0.816	0.820	0.702
17	0.381	8	0.789	776.2	68.08	708.1	489.85	0.866	0.806	0.672	0.651	0.623
17	0.381	15	0.768	1025.8	68.08	957.7	489.85	0.885	0.782	0.592	0.578	0.535

[a] $\sigma_i = \sigma_T - \sigma_c$. [b] $T_i^{calc} = \exp(-\sigma_i^B nd)$. [c] $T_i^{meas} = \exp(-\sigma_i nd)$.

in the final calculation of B. The difference between using T and T_i^{meas} varies between 1% and 3% whereas T_i^{calc} values are 4–23% larger than T_i^{meas}. T_i^{calc} values are closest for high deuterium content samples, and the error is largest for the lowest deuterium content samples. The measured transmissions, T, give values of the incoherent background that are always closer to the actual incoherent level than the use of T_i^{calc}, from bound atom values, throughout the range of deuterium contents and wavelengths used in this work. At low q where the coherent signal is large, the error in the estimation of the background is negligible (<0.1%). As the wavelength decreases, the cross section will approach the bound atom value; therefore, the use of σ_i^{calc} for measurements made at Oak Ridge, where $\lambda = 4.75$ Å, should not incur such large errors as it would in this work.

Another commonly used method of estimating the level of incoherent scattering is to assume that

$$I_{i,s} \propto \phi_H I_H + (1 - \phi_H) I_D$$

where the subscripts H and D refer to the hydrogenous and deuterated components, respectively. ϕ_H is the volume fraction of hydrogenous polymer. Strictly speaking this is only applicable if $T < 0.9$ so that, from eq 4, the scattered intensity

$$1 - T \approx n\sigma_T d$$

Thus the scattered intensity would be proportional to the number of scatterers or the volume fractions of the different scatterers. For the samples used in this work this method would overestimate the incoherent scattering from samples containing small amounts of deuterated polymer and underestimate it for samples containing a large proportion of deuterium. The discrepancy could be as high as 30%.

All the methods discussed here suffer from some drawbacks, and ideally the incoherent scattering should be measured directly, using polarization analysis. On balance, the use of the measured transmissions appears to produce less error.

Theory

The scattering from a blend composed of polymers 1 and 2 of which a proportion, c, of polymer 1 chains are deuterated is given by[17,18]

$$V_1 S(q) = \frac{[cd + (1-c)h - b']^2}{[F_1(q)]^{-1} + \beta[F_2(q)]^{-1} - 2\chi} + c(1-c)(d-h)^2 F_1(q) \quad (7)$$

where $F_i(q) = \phi_i N_i P_i(q)$ and ϕ_i, N_i, and $P_i(q)$ are the volume fraction, degree of polymerization, and single-chain scattering function of the ith component, respectively. The parameters d and h are the coherent scattering lengths of deuterated and hydrogenous polymer 1; and $b' = \beta b$, where b is the scattering length of polymer 2 and $\beta = V_1/V_2$. V_i is the molar volume of a monomer of polymer i; χ is the interaction parameter.

As it stands eq 7 is not very tractable; however, by a suitable choice of c, so that the numerator of the first term goes to zero, it can be reduced to

$$V_1 S(q) = c(1-c)(d-h)^2 \phi_1 N_1 P_1(q) \quad (8)$$

Thus the single-chain scattering function, which is related to R_1, the radius of gyration of polymer 1, can be measured without interference from the concentration fluctuation term.

When $c = 1$, χ may be obtained through eq 7, which reduces to

$$V_1 S(q) = \frac{(d - b')^2}{[\phi_1 N_1 P_1(q)]^{-1} + \beta[\phi_2 N_2 P_2(q)]^{-1} - 2\chi} \quad (9)$$

Rearranging eq 9 gives

$$\frac{(d-b')^2}{V_1 S(q)} = [\phi_1 N_1 P_1(q)]^{-1} + \beta[\phi_2 N_2 P_2(q)]^{-1} - 2\chi \quad (10)$$

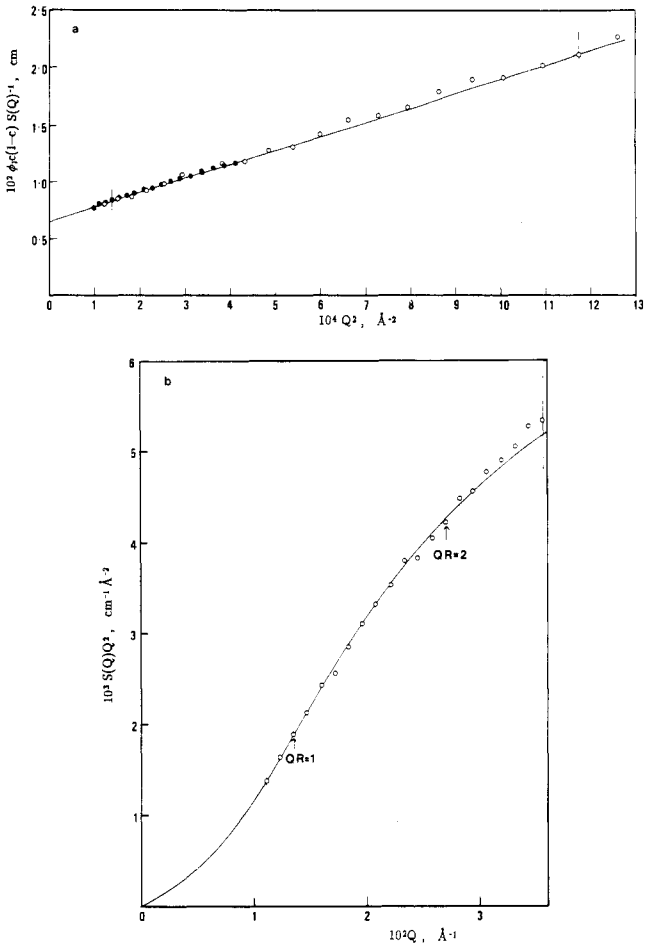

Figure 1. (a) Coherent scattered intensity, $S(q)$, from sample 11 (P4MS-*d* in P4MS) plotted according to eq 8: (○) data from D17; (●) data from D11. The line is the best fit to eq 8 using eq 12 for $P(q)$ with R = 74 Å and u = 0.73. Intercept = 0.66 × 10^{-2} cm. (b) The D17 data plotted as $S(q)q^2$ versus q.

χ can be estimated in two ways: (1) at $q = 0$, $P_i(q) = 1$, and eq 10 reduces to

$$\frac{(d - b')^2}{V_1 S(0)} = [\phi_1 N_1]^{-1} + \beta[\phi_2 N_2]^{-1} - 2\chi \qquad (11)$$

and therefore, if ϕ_i and N_i are known, χ can be estimated by extrapolating the data to $Q = 0$; (2) if $P_1(q)$ and $P_2(q)$ are known, the whole scattering curve can be fitted to give χ.

Results

1. Radii of Gyration. (a) P4MS/PM2PO. In Figure 1a, two sets of data for sample 11 (P4MS-*d* in P4MS) are plotted according to eq 8. The agreement between the data from D11 and D17 is excellent. The data have been fitted using the Debye equation for a Gaussian coil for $P(q)$ in eq 8 taking account of the polydispersity of the sample, i.e.

$$P(q) = \frac{2}{(u + 1)v^2}[(1 + uv)^{-1/u} - 1 + v] \qquad (12)$$

where $u = M_w/M_n - 1$ and $v = R^2q^2/(1 + 2u)$. R^2 is the mean-squared z-average radius of gyration. The fitted value for the radius of gyration is 74 Å. In Figure 1b the D17 data are plotted in the form of a Kratky plot, $S(q)q^2$ versus q; it is apparent from this plot that the data cover what is essentially the intermediate q range; i.e., $qR > 1$.

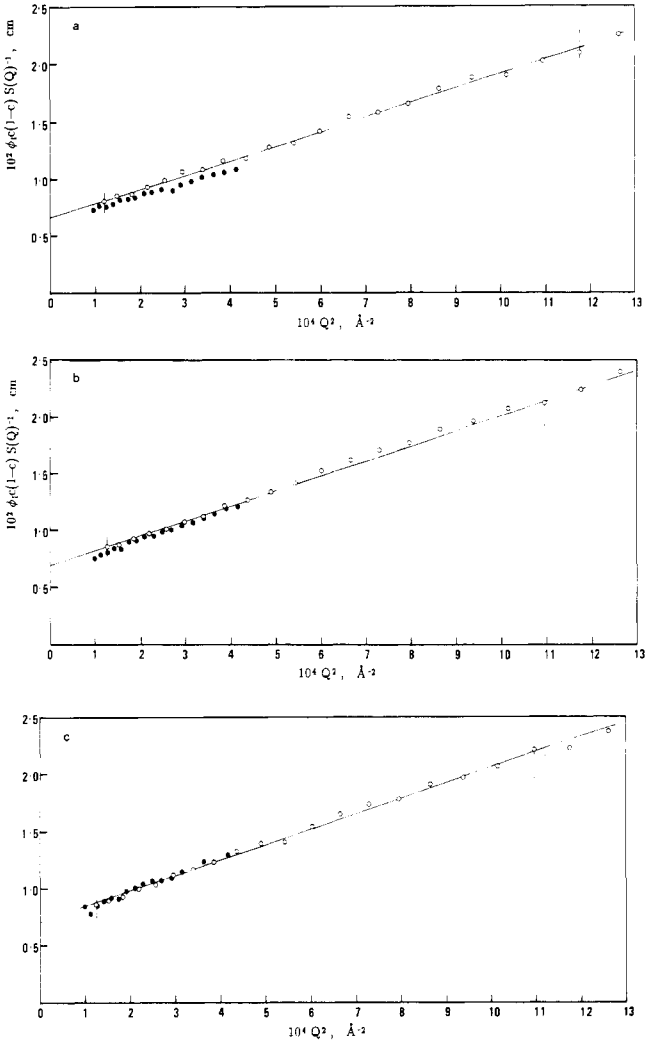

Figure 2. Coherent scattered intensity $S(q)$ plotted according to eq 8: (○) 260 °C (D17); (●) 220 °C (D11). The line is the best fit to eq 8 using eq 12 for $P(q)$ with R = 74 Å and u = 0.73: (a) sample 5, ϕ_{P4MS} = 0.611, intercept = 0.67 × 10^{-2} cm; (b) sample 7, ϕ_{P4MS} = 0.410, intercept = 0.70 × 10^{-2} cm; (c) sample 9, ϕ_{P4MS} = 0.209, intercept = 0.72 × 10^{-2} cm.

Above $qR = 2$ the data begin to approach the plateau region of the Debye curve. The fit of the data to the Debye curve is very good up to $q \sim 3 \times 10^{-2}$ Å^{-1}. At larger q values, the data are sensitive to any errors in background subtraction and any effects of local chain structure.

In Figure 2, the 260 °C data, measured on D17, from the blends of P4MS and PM2PO are plotted and fitted to eq 8. Equation 12 has been used for $P(q)$, and the same parameters that were used for the homopolymer mixture (P4MS-*d* in P4MS) have been used again for all the blends; i.e., a radius of gyration of 74 Å fits all three blend compositions and the homopolymer mixture. Also plotted on the same figures are the data from samples annealed at 220 °C, which were measured on D11 and cover a much narrower q range. The data from samples 7 and 9 fall either on or very close to the 260 °C data. Sample 5 shows a slight shift but is still within the estimated errors.

Inspection of the intercepts in Figure 2 shows that there is a small but systematic shift to higher values of $\phi_1 c(1 - c)\ S(0)^{-1}$ as ϕ_1, the volume fraction of P4MS, decreases (i.e., to lower apparent molecular weight). The shift in the intercept varies from +1.5% (ϕ_1 = 0.611) to +9% (ϕ_1 = 0.209). There are a number of possible errors that may be the cause, but all except one can be eliminated. Assuming that the analysis of data for homopolymer mixture

11 (P4MS-*d*/P4MS) has been correctly carried out, then the data from the three blends, 5, 7, and 9, should have the same intercept as each other and the homopolymer mixture. The discrepancy cannot be accounted for by assuming there is an error in the background subtraction since in most cases adjusting the flat background to obtain the same intercept as the homopolymer mixture would result in a *negative* amount of incoherent scattering being subtracted. Another more likely source of error is the value of c. This has been chosen so that the first term in eq 7 is approximately equal to zero, but since it is not exactly zero, there is a contribution from this term. It is possible, using the data from the measurements of χ (see the following section), to calculate the size of this first term exactly. This has been done and accounts for <0.2% of the total scattered intensity and would increase $S(0)$ and thus decrease the intercept relative to the homopolymer data. A closer inspection of the weight fraction of P4MS-*d* shows that they are small, between 4 and 13%. Each sample mixture was made up individually, and the maximum systematic rounding up error involved in weighing out these small amounts of deuterated material can be estimated. The resultant error in $c(1 - c)$ is calculated to be +6, +3, and +2% for samples 9, 7, and 5, respectively. Thus the intercepts when adjusted for the systematic error in c would be 0.66×10^{-2}, 0.68×10^{-2}, and 0.68×10^{-2} cm for samples 5, 7, and 9, respectively, compared to 0.66×10^{-2} cm for the homopolymer mixture, 11, giving a variation in the intercept of ±2%.

The value of the molecular weight measured by SANS, assuming the P4MS-*d* was 100% ring-deuterated, was 79% of the GPC value, well outside the estimated error of ±10%. This reduction in apparent molecular weight could be due to incomplete deuteration or possibly, calibration errors. The measured intercept implies that the rings are 90% deuterated on average (i.e., P4MS-$d_{6.3}$ not d_7). It is unlikely that the discrepancy is due to calibration errors as the data were collected from two spectrometers on three separate occasions. The method used to produce ring-deuterated polystyrenes uses H–D exchange, which does not necessarily result in 100% substitution of the H atoms by the D atoms. Unfortunately, the amount of pure deuterated polymer available after the SANS measurements precluded any IR or NMR measurements to check the level of deuteration. The effect of assuming incomplete deuteration on the measured interaction parameters is discussed further in section 2a.

(b) PS/PM2PO. In Figure 3a two sets of data for sample 21, PS-*d*/PS, are plotted according to eq 8. The agreement between the D17 and D11 data is reasonable although not as good as for the P4MS-*d*/P4MS sample. The data have been fitted using eq 12 and a value for R of 173 Å. The fit of the data to the Debye curve is good at low q but becomes increasingly less good at high q. This can be seen more clearly in Figure 3b where the D17 data are plotted as $S(q)q^2$ versus q. The intensity has a tendency to be too high at high q, indicating a possible error in the background subtraction or that PS-d_5 does not conform to the Debye form for a Gaussian. Changing the value of u, the polydispersity index, in eq 9 cannot account for the increase in $S(q)$. All the data lie in the intermediate q range ($qR > 1$).

In Figure 4, the 220 and 260 °C data for four blends of PS and PM2PO are plotted. Each set of data has been fitted with the same value of R, 173 Å. Again, the fit to the Debye function is good at low q. The 220 and 260 °C are essentially indistinguishable except for sample 20, which shows some difference between the two sets of data,

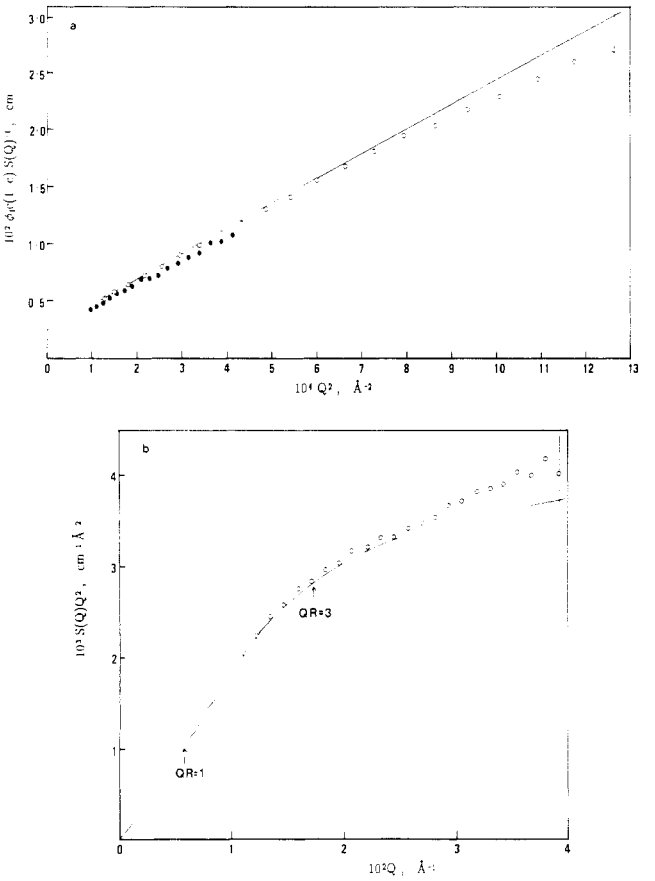

Figure 3. (a) Coherent scattered intensity, $S(q)$, from sample 21 (PS-*d* in PS) plotted according to eq 8: (○) data from D17; (●) data from D11. The line is the best fit to eq 8 using eq 12 for $P(q)$ with R = 173 Å and u = 1.94. Intercept = 0.24×10^{-2} cm. (b) The D17 data plotted as $S(q)q^2$ versus q.

although this is still within the estimated errors. There is no measurable variation of R with temperature or composition.

Inspection of the intercepts in Figure 4 compared to that in Figure 3 for PS-*d*/PS shows the same systematic shift as seen in the data for P4MS/PM2PO. However, in this case, the shifts are much larger as the amount of deuterated material is much smaller. The intercepts vary from 0.24×10^{-2} cm for the homopolymer mixture, 21, to 0.31×10^{-2} cm for sample 20 ($\phi_{PS\text{-}d} = 0.018$). Estimation of the systematic error in $c(1 - c)$ adjusts the values of the intercepts for samples 14, 16, 18, and 20 to 0.23×10^{-2}, 0.25×10^{-2}, 0.25×10^{-2}, and 0.24×10^{-2} cm, respectively, giving a variation in the estimated molecular weight of ±4%.

The molecular weight calculated assuming that the PS-*d* was fully ring-deuterated was found to be considerably lower than the GPC value, as it had been for P4MS-*d*. The difference between the SANS and GPC values was even greater, the SANS value being only 73% of the GPC value. This value also indicates a level of deuteration of about 90% (i.e., $d_{4.4}$ not d_5).

2. Interaction Parameters. (a) P4MS-*d*/PM2PO. In Figure 5 the data from sample 6 annealed at 260 °C are plotted according to eq 10. The value of d, the scattering length of P4MS-*d*, used in the calculation is the value obtained from the single-chain measurements using the GPC measured molecular weight. It has been assumed that the polymer is not fully deuterated. If, however, the discrepancy between the SANS and GPC measured molecular weights is attributed to calibration errors, then the scattering from the homopolymer could be used to normalize the data. This method would result in the χ values

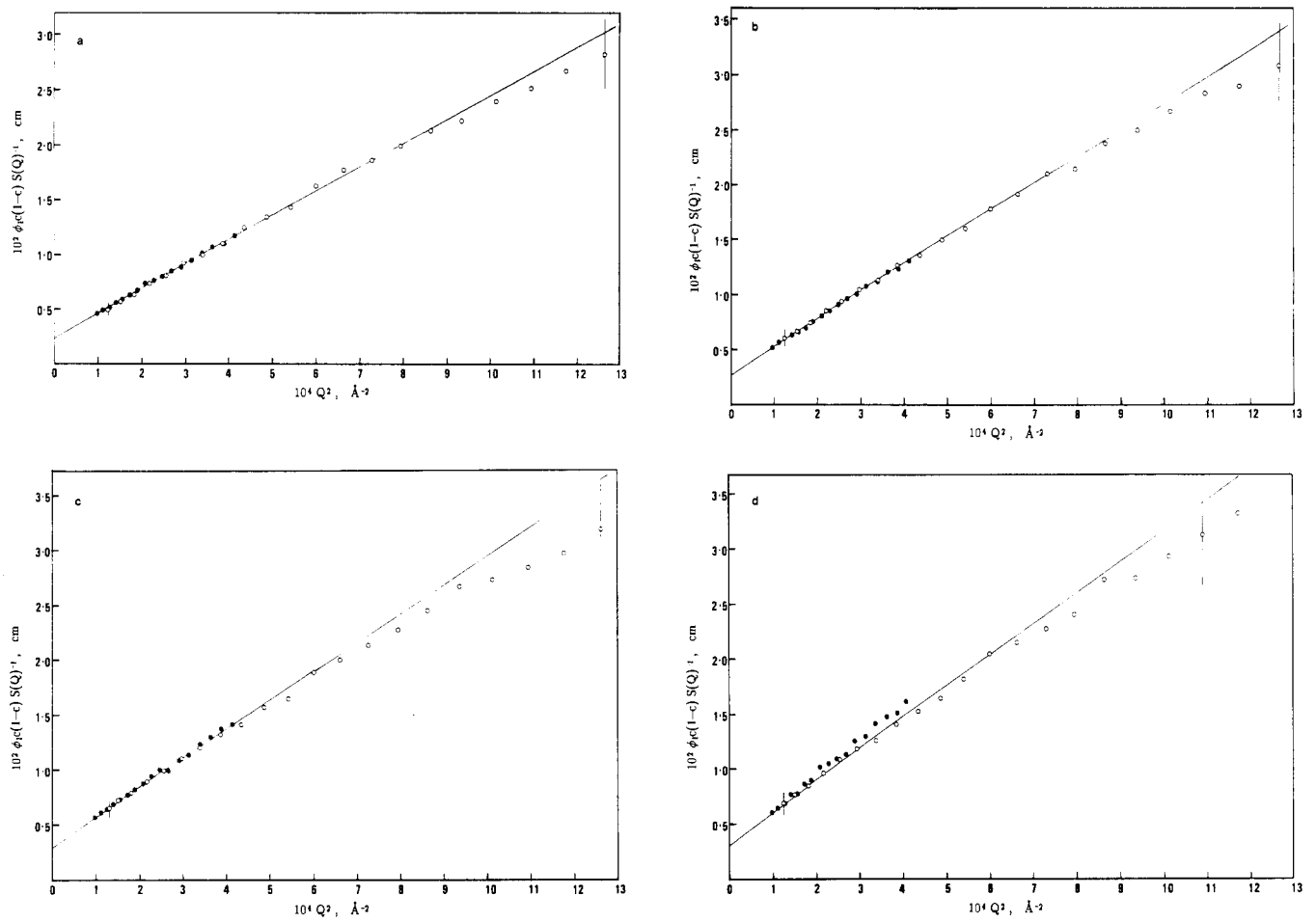

Figure 4. Coherent scattered intensity, $S(q)$, plotted according to eq 8: (○) 260 °C (D17); (●) 220 °C (D11). The line is the best fit to eq 8 using eq 12 for $P(q)$ with R = 173 Å and u = 1.94; (a) sample 14, ϕ_{PS} = 0.802, intercept = 0.24 × 10^{-2} cm; (b) sample 16, ϕ_{PS} = 0.602, intercept = 0.27 × 10^{-2} cm; (c) sample 18, ϕ_{PS} = 0.402, intercept = 0.29 × 10^{-2} cm; (d) sample 20, ϕ_{PS} = 0.202, intercept = 0.31 × 10^{-2} cm.

being 1–2% smaller, well within the estimated experimental error. There is no reason to suspect the GPC values particularly since the polystyrenes were measured on two different instruments and the values agreed to within 10%. Neutron scattering is very sensitive to the level of deuteration.

The plot in Figure 5 is curved; therefore, χ has been estimated assuming thermodynamic equilibrium by fitting the data to eq 10 using the Debye equation for P_1 and P_2 with measured values for R_1 and R_2. The values of the radii of gyration that have been used are 74 Å for P4MS and 88 Å for PM2PO.[19] In Figure 5 the same data are shown with the calculated equilibrium curves for $\chi = 0$ and $\chi = -1.54 \times 10^{-2}$. It is now evident that the curvature is due to excess intensity at low q. Extrapolating the low-q data to give $S(0)$ would lead to a larger, less negative value for χ.

In Figure 6 the data from the other compositions at 260 °C are plotted. The excess intensity at low q increases with increasing P4MS-d content and therefore decreasing glass transition temperature. The annealing time also decreases with increasing P4MS-d content. This excess intensity is not apparent in the single-chain specimens for which the concentration fluctuation term is zero. The values of χ obtained from these data plus values obtained at other annealing temperatures are listed in Table IV. Inspection of Table IV shows that although there is quite a large variation of χ with composition, there is little variation with temperature. With the exception of sample 33 (the sample with the lowest T_g) any variation of χ with temperature is zero within the estimated error.

Table IV
Values of the Interaction Parameter χ for the Blend P4MS-d/PM2PO

			$\chi \times 10^2$ (±16%)			
sample	ϕ_{P4MS-d}	T_g, K	493 K[a]	513 K[a]	533 K[a]	553 K[a]
33	0.101	473	−1.05		−0.78	
8	0.198	460		−0.70	−0.68	−0.60
34	0.301	449	−1.17		−1.25	
6	0.399	437			−1.54	
4	0.600	417			−2.04	

[a] Annealing temperature ±1 K.

(b) PS-d/PM2PO. The data for the PS-d/PM2PO blends annealed at 260 °C are plotted according to eq 10 in Figure 7. The same procedure was used for calculating d, the coherent scattering length of PS-d, as has been used for P4MS-d assuming partial deuteration. The values of χ have been estimated by fitting the data in the high-q region. At low q there is excess intensity, which increases as the proportion of PS-d increases. The effect is particularly marked in Figure 7e where the volume fraction of deuterated polymer is 0.584. For this sample only an estimate of the lower limit of the size of the χ parameter can be made as the curvature extends across almost the entire q range. The χ parameters obtained from these data plus those obtained at other annealing temperatures are listed in Table V. As already observed for the P4MS-d/PM2PO blends, there is little variation of χ with temperature, but χ appears to vary with composition.

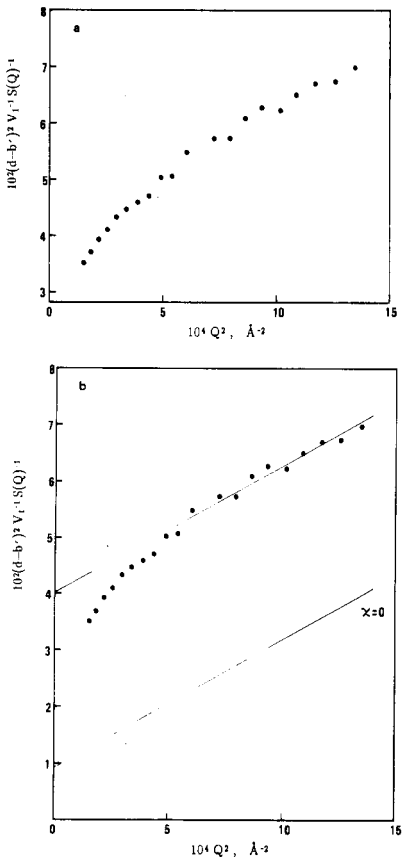

Figure 5. (a) Typical set of data from a P4MS-*d*/PM2PO blend, sample 6, ϕ_{P4MS-d} = 0.399 at 260 °C. The data are plotted according to eq 10. The value of d used was obtained from the intercept of Figure 1 assuming M_w = 88 500. (b) The same data as a. The lines are calculated according to eq 10 assuming R_1 = 74 Å and R_2 = 88 Å with appropriate values of ϕ_i, N_i, and u_i (see Table I).

Table V
Values of the Interaction Parameter χ for the Blend PS-*d*/PM2PO

			χ × 10² (±16%)			
sample	ϕ_{PS-d}	T_g, K	493 K[a]	513 K[a]	533 K[a]	553 K[a]
31	0.094	472	−2.1		−2.12	
19	0.198	459			−2.07	
32	0.288	446	−2.27		−2.42	
17	0.381	435		−2.93	−2.88	−2.90
15	0.584	414			(−4.1)	

[a] Annealing temperature ±1 K.

Discussion

The single-chain measurements for both blends show that they are homogeneous, single-phase systems. Neither the radii of gyration nor the apparent molecular weights of PS-*d* or P4MS-*d* changes on mixing with PM2PO. Composition and temperature independence of the radii of gyration of one of the blend components has also been observed in other systems.[20,21] The interaction parameters for the two systems are large and negative although they are less favorable for the P4MS-*d*/PM2PO blends than for the PS-*d*/PM2PO blends of equivalent composition. This is not surprising as it is known that chlorination[4] or bromination[7] of one of the components of PS/PM2PO blends can cause reduction in miscibility and eventually phase separation. However, the addition of a methyl group in the para position on the phenyl ring does not seem to produce such a large effect as halogenation since the blend is still miscible over a wide composition range.

What is surprising is the apparent lack of any *temperature* dependence of the interaction parameters. If the values of χ, for sample 17, are extrapolated to χ_s, the spinodal value, then the predicted spinodal temperature is −370 K, clearly impossible. Thermodynamics dictates that, as the temperature of a polymer mixture changes, then so must χ, the interaction parameter. Whether χ decreases or increases with increasing temperature will depend upon whether the system exhibits an upper or lower critical solution temperature. The system PS/PM2PO is known to exhibit all the signs associated with a system that has an LCST,[1] even though it has not actually been observed to phase separate. The temperature dependence of χ at infinite dilution for the system deuterated PM2PO (PM2PO-*d*)/PS has been measured by Maconnachie et al.[1] (PXE-*d* in ref 1 ≡ PM2PO-*d*). Assuming, for the moment, that PS-*d*/PM2PO at finite concentrations behaves similarly to PM2PO-*d*/PS, then χ(240 °C) and χ(280 °C) would be of the order of -3.1×10^{-2} and -2.0×10^{-2}, respectively; therefore, over 40 deg there should be a significant change in χ.

The SANS measurements on the PM2PO-*d*/PS system were carried out on samples that were held at the actual temperature of the measurements for at least 1 h. The samples were not quenched. The method used to produce the specimens for this work involved annealing followed by quenching. The annealing times varied from 10 to 90 min depending upon the difference between the annealing temperature and the glass transition temperature, T_g. The minimum difference, ΔT (=$T - T_g$), was 20 deg, and the largest difference was 120 deg. At the highest values of ΔT the samples flowed easily so that equilibrium at the annealing temperature should have been established rapidly. Even at the lowest ΔT values, annealing times should have been sufficiently long (~90 min) for equilibrium to be established. In order to check whether or not this assumption was correct, two samples were annealed for different lengths of time up to 6 h and quenched and their scattering patterns compared. No effect of annealing time was observed. It was therefore assumed that the samples had equilibrated at the annealing temperature. However, the almost identical χ values at high q would imply that the samples "equilibrated" at the *same* temperature and not at the various annealing temperatures.

The effect of quenching or cooling rate on the scattering from PS-*d*/PM2PO blends has been predicted by Kramer and Sillescu.[23] Their calculated plots of $S(q)^{-1}$ versus q^2, are curved at low q and follow the shape of the equilibrium scattering curve at high q. As q tends to zero, the value of χ measured by extrapolating the data to q = 0 should be close to that associated with the annealing temperature. At higher q the χ values approach that expected at T_g. Their calculations imply that unless the samples are at temperatures very close to T_g then it is impossible to quench them rapidly enough to obtain the equilibrium scattering curves for the annealing temperature. Qualitatively the data presented in this paper behave in a similar manner to that predicted by Kramer and Sillescu. However, the q range covered by our data is much wider, and our values of χ are obtained at high q; thus, if the trends shown by the calculated curves are correct, they are closer to those expected at T_g *not* at the annealing temperatures.

Recently, Composto et al.[2] have reported on the mutual diffusion of fully deuterated PS/PM2PO blends in which they showed that χ did not vary with composition over a wide range of compositions. As part of this work they examined previous SANS measurements[1,3,7,22] on fully deuterated PS/PM2PO blends and found that they could

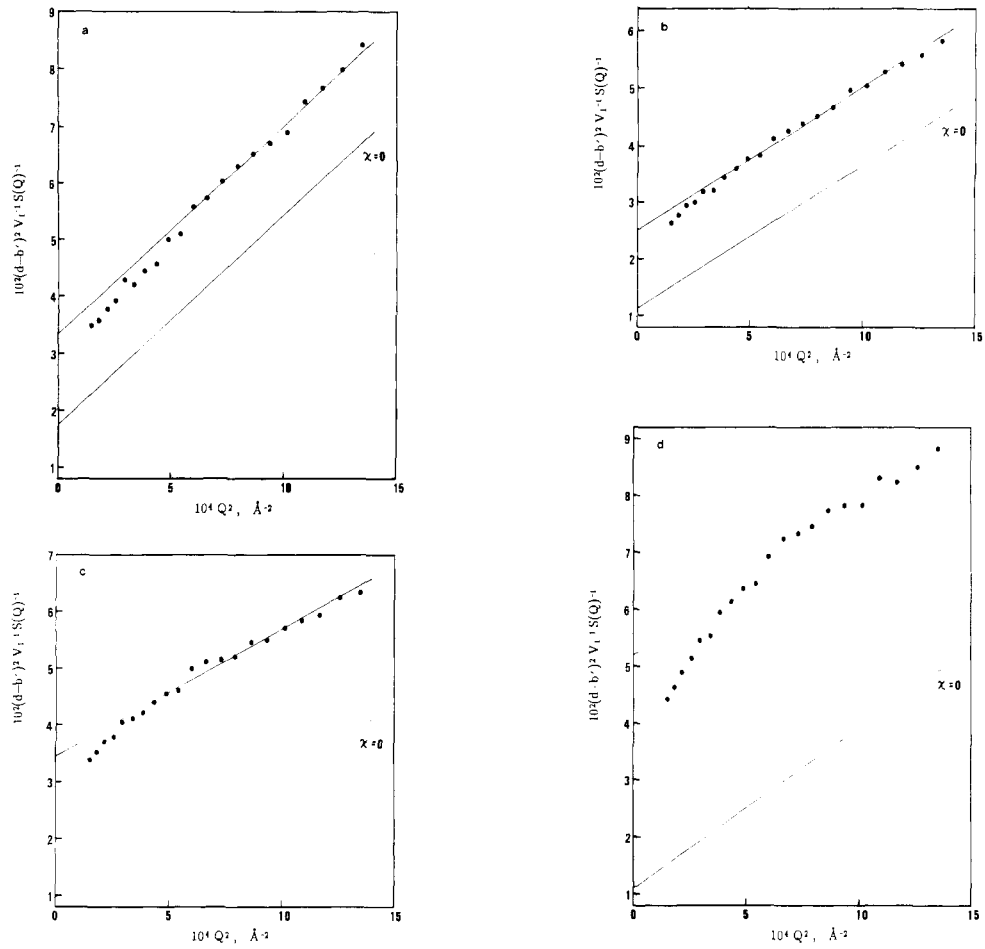

Figure 6. Data from the other blends of P4MS-*d*/PM2PO at 260 °C plotted according to eq 10. The lines through the data were calculated assuming $R_1 = 74$ Å and $R_2 = 88$ Å with the appropriate values of ϕ_i, N_i, and u_i (see Table I): (a) $\phi_{P4MS\text{-}d} = 0.101$, $\chi = -0.78 \times 10^{-2}$; (b) $\phi_{P4MS\text{-}d} = 0.198$, $\chi = -0.68 \times 10^{-2}$; (c) $\phi_{P4MS\text{-}d} = 0.301$, $\chi = -1.25 \times 10^{-2}$; (d) $\phi_{P4MS\text{-}d} = 0.600$, $\chi = -2.04 \times 10^{-2}$.

fit nearly all the data, together with their mutual diffusion measurements, with the same temperature dependence. By considering the rate at which the SANS samples were cooled or quenched, they assigned a temperature at which the systems equilibrated[2] using the method of Kramer and Sillescu.[23] The faster the cooling rate, the more curvature would be expected at low q. In the present experiments the cooling rate was not monitored, but quenching probably occurred within 30 s.

The calculated scattering curves of Kramer and Sillescu appear to show that at high q the data approach that expected for a sample equilibrated close to T_g, i.e., that over small distances the samples can equilibrate very rapidly as they are quenched. Figure 8 shows a plot of χ versus T_g^{-1} for PS-*d*/PM2PO where it has been assumed that the samples equilibrated at high q close to their T_g's and *not* at the annealing temperatures and that there is no composition dependence of χ as proposed in ref 2. The line drawn through the data is the temperature dependence measured by Composto et al.[2], $\chi = 0.112 - 62/T$ (K); the correlation is remarkable. When the same argument is used for the P4MS-*d*/PM2PO data, Figure 9 shows the results of plotting χ versus T_g^{-1}, assuming no composition dependence. The line drawn through the data is a least-squares fit, $\chi = 0.098 - 49/T$ (K). The other part of the argument proposed by Kramer and Sillescu implies that extrapolation of the data to zero q would produce values of χ that related to the original annealing temperature. Unfortunately the range of q covered by our data is insufficient to give a very accurate assessment of the intensity of zero q. However extrapolation of the data from the PS/PM2PO system predicts, for three of the samples, that the average equilibrium temperature at low q is approximately 500 K compared with an annealing temperature of 533 K. For P4MS/PM2PO the same method would predict an average temperature of about 470 K. Although the extrapolations are inaccurate, the predicted temperatures are tending toward the annealing temperatures. Curved plots of $S(q)^{-1}$ versus q^2 have been fitted with quadratic functions to obtain $S(0)$ and thus χ by a number of authors (see for example ref 24 and 25). Higgins et al.[25] correlated the values of χ, which they obtained using this method to values obtained in the two-phase region of the phase diagram. This would seem to confirm that at zero q χ relates to the annealing temperature. The shape of the curves is indicative of nonequilibration of the blends.

In Figure 8 the temperature dependence of χ for the system PM2PO-*d*/PS from ref 1 is also plotted. There is a shift to less negative χ values for this blend. The temperature dependence proposed by Composto et al.[2] appears to hold for both fully deuterated PS/PM2PO and the samples used in this work, which are ring-deuterated PS/PM2PO blends. The difference between the two curves might imply that the interactions between PS and PM2PO are much more sensitive to changes in PM2PO than in PS. Deuterating the PS backbone does not affect the interactions between the polymers at all, which would be consistent with the work that advocates an interaction between the phenyl and phenylene rings.[26] The difference in the magnitude of the interaction parameters between P4MS-*d*/PM2PO and PS-*d*/PM2PO is less than that

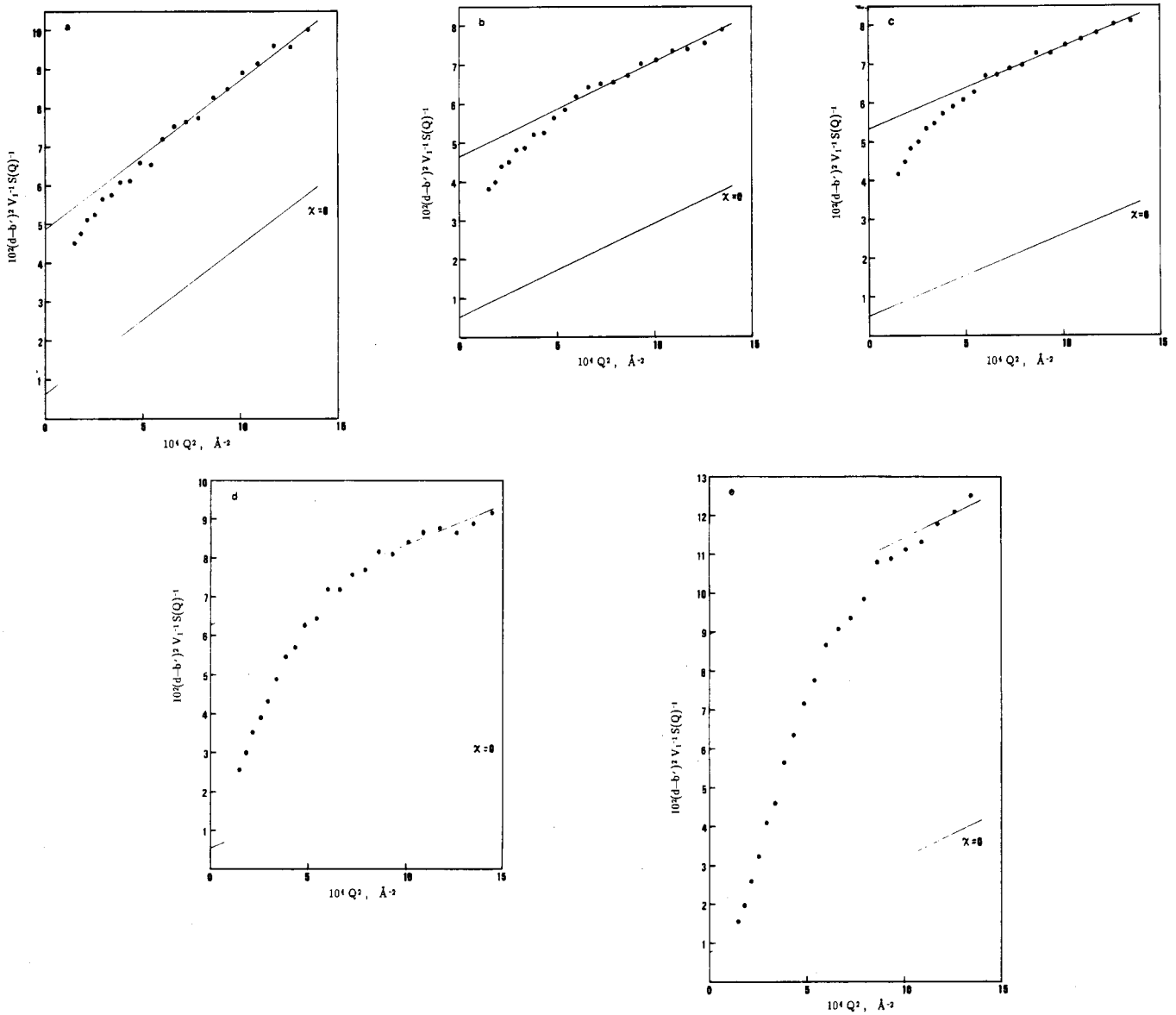

Figure 7. Data from the blends of PS-*d*/PM2PO at 260 °C plotted according to eq 10. The lines through the data were calculated assuming R_1 = 173 Å and R_2 = 88 Å with the appropriate values of ϕ_i, N_i, and u_i (see Table I): (a) $\phi_{PS\text{-}d}$ = 0.094, $\chi = -2.12 \times 10^{-2}$; (b) $\phi_{PS\text{-}d}$ = 0.198, $\chi = -2.07 \times 10^{-2}$; (c) $\phi_{PS\text{-}d}$ = 0.288, $\chi = -2.42 \times 10^{-2}$; (d) $\phi_{PS\text{-}d}$ = 0.381, $\chi = -2.88 \times 10^{-2}$; (e) $\phi_{PS\text{-}d}$ = 0.584, $\chi = -4.1 \times 10^{-2}$.

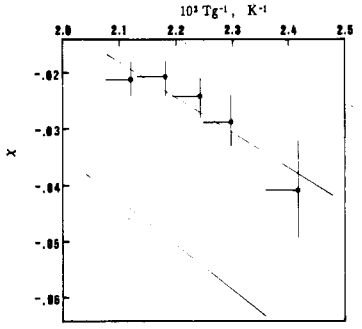

Figure 8. Plot of χ versus T_g^{-1} for the PS-*d*/PM2PO blends. The horizontal lines delineate the temperature range T_g to T_g + 10 deg. The line drawn through the data is from ref 2 where $\chi = 0.112 - 62/T$. The lower line is that measured for the system PM2PO-*d*/PS from ref 1 where $\chi = 0.121 - 78/T$.

between PS-*d*/PM2PO and PM2PO-*d*/PS blends.

Conclusions

The two blends PS-*d*/PM2PO and P4MS-*d*/PM2PO exhibit similar behavior although there is a significant shift

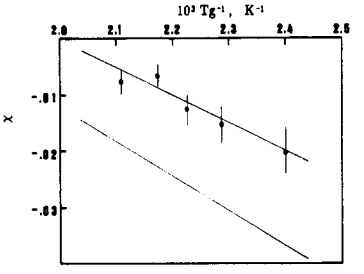

Figure 9. Plot of χ versus T_g^{-1} for the blends P4MS-*d*/PM2PO. The line through the data is a least-squares fit where $\chi = 0.098 - 49/T$. The lower line is the temperature dependence exhibited by PS-*d*/PM2PO blends from ref 2 for comparison.

to less favorable χ parameters for the P4MS-*d*/PM2PO system. The conformation of the deuterated polymers does not vary with composition in both blends. There is no evidence of any measurable chain expansion or contraction of the PS or P4MS.

The present work suggests a number of different approaches to obtaining interaction parameters from SANS measurements. If samples are annealed close to T_g and

then quenched, the equilibrium scattering curve is more likely to be measured so that all the data can be used to obtain χ. If the data are obtained at low q, then extrapolation to zero q should result in χ values that relate to the annealing temperature. However, at high q the values of χ will tend toward those associated with temperatures closer to T_g. If measurements are made on unquenched samples, which are equilibrated at the measuring temperature, no ambiguities should arise.

Finally, the evidence from this work that the PS/PM2PO system shows no composition dependence of χ supports that from mutual diffusion measurements.[2]

Acknowledgment. We thank our local contact at the Institut Laue-Langevin, Dr. A. Rennie, for his assistance. J.R.F. thanks the NSF and the SERC for Visiting Fellowships. P.E.T. thanks the SERC for support during the period of this work. We are grateful to Prof. E. Kramer for very helpful discussions and for allowing us to see ref 2 and 23 before publication.

Registry No. PS, 9003-53-6; PM_2PO, 24938-67-8; P_4MS, 24936-41-2; neutron, 12586-31-1.

References and Notes

(1) Maconnachie, A.; Kambour, R. P.; White, D. M.; Rostami, S.; Walsh, D. J. *Macromolecules* **1984**, *17*, 2645.
(2) Composto, R. J.; Kramer, E. J.; White, D. M. *Macromolecules* **1988**, *21*, 2580.
(3) Jelenic, J.; Kirste, R. G.; Oberthür, R. C.; Schmitt-Strecker, S.; Schmitt, B. J. *Makromol. Chem.* **1984**, *185*, 129.
(4) Fried, J. R.; Karasz, F. E.; MacKnight, W. J. *Macromolecules* **1978**, *11*, 150.
(5) Vukovic, R.; Karasz, F. E.; MacKnight, W. J. *J. Appl. Polym. Sci.* **1983**, *28*, 219.
(6) Vukovic, R.; Karasz, F. E.; MacKnight, W. J. *Polymer* **1983**, *24*, 529.
(7) Maconnachie, A.; Kambour, R. P.; Bopp, R. C. *Polymer* **1984**, *25*, 357.
(8) Fried, J. R.; Lorenz, T.; Ramdas, A. *Polym. Eng. Sci.* **1985**, *25*, 1048.
(9) Dickinson, L. C.; Yang, H.; Chu, C.-W.; Stein, R. S.; Chien, J. C. W. *Macromolecules* **1987**, *28*, 1757.
(10) Maier, B., Ed. *Neutron Research Facilities at the ILL High Flux Reactor*; Institut Laue-Langevin: Grenoble, France, 1983.
(11) Ragnetti, M.; Geiser, D.; Höcker, H.; Oberthür, R. C. *Makromol. Chem.* **1985**, *186*, 1701.
(12) Hayashi, H.; Flory, P. J.; Wignall, G. D. *Macromolecules* **1983**, *16*, 1328.
(13) Rawiso, M.; Duplessix, R.; Picot, C. *Macromolecules* **1987**, *20*, 630.
(14) Gawrisch, W.; Brereton, M. G.; Fischer, E. W. *Polym. Bull.* **1981**, *4*, 687.
(15) Maconnachie, A. *Polymer* **1984**, *25*, 1068.
(16) O'Reilly, J. M.; Teegarden, D. M.; Wignall, G. D. *Macromolecules* **1985**, *18*, 2747.
(17) de Gennes, P.-G. *Scaling Concepts in Polymer Physics*; Cornell University Press: Ithaca, NY, 1979.
(18) Warner, M.; Higgins, J. S.; Carter, A. J. *Macromolecules* **1983**, *16*, 1931.
(19) Reanalysis of the data from ref 1 gives a value of R for PM2PO-d in PM2PO of 88 Å, not 100 Å as originally published.
(20) Tomlins, P. E.; Higgins, J. S. *Macromolecules* **1988**, *21*, 425.
(21) Bates, F. S.; Fetters, L. J.; Wignall, G. D. *Macromolecules* **1988**, *21*, 1086.
(22) Wignall, G. D.; Child, H. R.; Li-Aravena, F. *Polymer* **1980**, *21*, 131.
(23) Kramer, E. J.; Sillescu, H. *Macromolecules* **1989**, *22*, 414.
(24) Murray, C. T.; Gilmer, J. W.; Stein, R. S. *Macromolecules* **1985**, *18*, 996.
(25) Higgins, J. S.; Fruitwala, H.; Tomlins, P. E. *Macromolecules*, in press.
(26) Wellinghoff, S. T.; Koenig, J. L.; Baer, E. *J. Polym. Sci., Polym. Phys. Ed.* **1977**, *15*, 1913.

Monomer and Polymers Derived from 2,6-Bis((dimethylamino)formyl)-4-(diallylamino)pyridine

Lon J. Mathias,* Teresa Kloske, and Gustavo Cei

Department of Polymer Science, University of Southern Mississippi, Southern Station Box 10076, Hattiesburg, Mississippi 39406-0076. *Received April 6, 1989*

ABSTRACT: A new metal complexing polymer has been synthesized. The corresponding monomer and model compounds are obtained from 4-hydroxypyridine-2,6-dicarboxylic acid (chelidamic acid). The monomer is a diallylamine derivative that can be cyclopolymerized with free radical initiators in aqueous acid. Similar to other diallylamines, it yields a linear and water-soluble polymer. The complexing activity is due to the pyridine nitrogen along with amide functions in positions 2 and 6. These provide not only a chelating effect that strongly enhances the complex stability but also the possibility of different binding geometries as suggested by changes in the solution NMR spectra upon addition of diverse transition-metal salts. This variability is probably responsible for the ability to complex metals that bind to the ligand in different preferred ways.

Introduction

4-(Dialkylamino)pyridines have been used as nucleophilic catalysts for several years. The range of applications has been the object of several reviews.[1-3] The most commonly used derivative is 4-(dimethylamino)pyridine (DMAP, below) due to both high efficiency in a number of reactions and low price. Although 4-pyrrolidinopyridine (PPY, below) has been reported to be in several cases more effective than DMAP,[2] its use has been restricted due to its higher price.

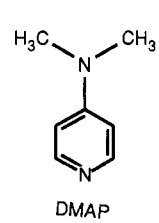

DMAP

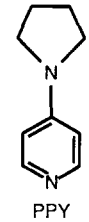

PPY

We have been involved for several years in the synthesis and characterization of polymers containing PPY units in the backbone.[4,5] 4-(Diallylamino)pyridine (DAAP) was synthesized and shown to polymerize by a free radical mechanism yielding a non-cross-linked, water-soluble polymeric catalyst (below) whose activity is superior to that

0024-9297/89/2222-4615$01.50/0